Iris Synthesis: A Reverse Subdivision Application

Lakin Wecker*
Department of Computer Science
University of Calgary
2500 University Drive NW
Calgary, Alberta
T2N 1N4

Faramarz Samavati†
Department of Computer Science
University of Calgary
2500 University Drive NW
Calgary, Alberta
T2N 1N4

Marina Gavrilova‡
Department of Computer Science
University of Calgary
2500 University Drive NW
Calgary, Alberta
T2N 1N4

Abstract

Due to renewed interest in security, iris images have become a popular biometric alternative to fingerprints for human identification. However, there exist very few databases on which researchers can test iris recognition technology. We present a novel method to augment existing databases through iris image synthesis. A multiresolution technique known as reverse subdivision is used to capture the necessary characteristics from existing irises, which are then combined to form a new iris image. In order to improve the results, a set of heuristics to classify iris images is proposed. We analyze the performance of these heuristics and provide preliminary results of the iris synthesis method.

CR Categories: I.3.3 [Computing Methodologies]: Computer Graphics—Picture/Image Generation; I.4.10 [Image Processing and Computer Vision]: Image Representation—Hierarchical; I.5.4 [Pattern Recognition]: Applications—Computer Vision; J.3 [Computer Applications]: Life and Medical Sciences—Biology and Genetics

Keywords: biometrics, biometric synthesis, multiresolution, reverse subdivision, image generation

1 Introduction

Biometrics conventionally involves the analysis of biometric data for identification purposes. Due to logistical and privacy issues with collecting and organizing large amounts of biometric data, a new direction of biometric research concentrates on the synthesis of biometric information. One of the primary goals of the synthesis of biometric data is to provide databases on which the classical biometric algorithms can be tested [Yanushkevich et al. 2004]. To facilitate identification with iris images, most recognition methods use a wavelet transform to encode a set of iris features, which can then be compared using different measures. There exists some research on the various wavelet transforms and related comparison methods [Wildes and Asmuth 1994; Huang et al. 1997; Zhu et al. 2000; Daugman 2004], however there are only a few works in the area of iris image synthesis [Lefohn et al. 2003; Cui et al. 2004].

*e-mail: weckerl@cpsc.ucalgary.ca
†e-mail: samavati@cpsc.ucalgary.ca
‡e-mail: marina@cpsc.ucalgary.ca

In this paper, we introduce a method to augment existing iris image databases through a novel iris generation technique. We present a multiresolution framework to decompose iris images into several components, and then recombine components of different irises into a new image. By using components of real irises in our synthesis method we are able to synthesize iris images which are very realistic. Loosely speaking, this is similar to genetic inheritances, in which the irises of the children resemble those of the parents. Finally, we present results which demonstrate the effectiveness of our method in producing realistic iris images and increasing the size of iris databases.

1.1 Previous Work

Fingerprints have conventionally been the primary biometric used for human identification. Thus, fingerprint technology benefits from a large community of fingerprint experts and researchers. They also have well known classifications and properties which allow generation algorithms to target a smaller subset of the possible random variations. Cappelli et al. describes a complete system for human fingerprint image generation [2002]. Their system uses fingerprint classifications to generate the global shape of each fingerprint. This global shape then undergoes a series of deformations and random variations in order to achieve the master ridge patterns. Once the master ridge patterns are known, their system can generate multiple samples of the original image using combinations of deformations throughout the synthesis process. They validate their results by exploiting the ubiquity of fingerprint identification and the subsequent availability of fingerprint experts and competitions.

Lefohn et al. introduced a method to synthesize human irises for use in computer graphics applications [2003]. The method makes use of the domain knowledge of ocularists to obtain results which take on a high level of realism. Their approach uses 30-70 layers of painted textures, scanned into the program using a conventional flat bed scanner. The domain specific knowledge required to produce the textures, renders this approach overly complicated and thus unsuitable for our purposes.

Cui et al. proposed a method to synthesize iris images, based on principal component analysis (PCA) and super-resolution [2004]. Using their experimental results, they conclude that a 75 dimensional PCA global feature vector provides the most benefit to the performance of the PCA recognition method. The synthesis method uses the same size feature vector, and the problem is constrained to a search in a limited high dimensional space. Once a feature vector has been synthesized with this search, they use super-resolution to obtain an iris image of the desired size. Using their method they generated a database of ten thousand iris classes with fifty one iris images in each class. Their method is restricted to the search space represented by the PCA of global feature vectors. Unlike PCA, our method, multiresolution analysis, can capture both local and global features due to the properties of scaling and wavelets. In addition, multiresolution provides us with an efficient and easy implementation when compared with PCA which has greater computational

requirements. Furthermore, improving the realism of the synthetic irises is proposed as a future work in their paper while our method synthesizes very realistic irises in comparison with their results.

We propose to generate iris images as unique combinations of existing irises, and we also introduce heuristics used to classify iris images. We organize our paper as follows. In Section 2, we will give a short overview of multiresolution with reverse subdivision, and explain how we applied it to our domain. Section 4 is a description of the pre-processing and post-processing steps that we employ when processing iris images. Next, in Section 5.2, we propose some classifications for irises in order to separate these irises into sets with similar characteristics which improves the resulting image quality. In Section 5 we will describe the core method we used for iris synthesis and in Section 6 present the results we obtained. Finally, in Section 7 we will draw conclusions and suggest future work in the area.

2 Multiresolution with Reverse Subdivision For Iris Synthesis

Multiresolution methods and wavelets have been used extensively in biometric and other image processing areas; for iris identification [Daugman 2004; Huang et al. 1997; Wildes and Asmuth 1994; Zhu et al. 2000], for document contour extraction [Yang et al. 1999] as well as for handwritten numeral recognition [Sabourin et al. 2002]. Multiresolution methods conventionally employ wavelets to obtain an efficient and compact representation of the original data [Stollinitz et al. 1996]. Samavati and Bartels introduced a general method to obtain a multiresolution curve representation by reversing subdivision rules [1999]. This method uses least squares to ensure that the low resolution version of the data is a good representation for the high resolution model. They further improved this method by using local least squares to obtain local multiresolution filters for various subdivision methods [2000; 2004]. In this work we have used multiresolution filters of Chaikin subdivision. This subdivision is a discrete approximation of quadratic B-Spline while Haar wavelets are based on zero degree B-Splines (piecewise constant). Although Haar filters are simple their scaling and wavelet functions are not even continuous and higher degree B-Splines are preferred for our purposes [Unser 1997]. Chaikin reverse subdivision filters have been proposed as alternatives to the traditional Haar wavelets for applications in biometrics [Samavati and Bartels 2004].

A multiresolution representation allows us to represent data in terms of two new data sets: a coarse approximation of the original data and a higher frequency set of details of the original data. Multiresolution operations are typically expressed as matrix equations in terms of the filter matrices $\mathbf{A}^n$, $\mathbf{B}^n$, $\mathbf{P}^n$, and $\mathbf{Q}^n$ [Stollinitz et al. 1996]. Given a particular column vector, C^n, of data, we can find a low resolution approximation, C^{n-1}, by applying the equation:

$$C^{n-1} = \mathbf{A}^n C^n. \tag{1}$$

Similarly, we can find the high frequency details, D^{n-2}, by applying the equation:

$$D^{n-1} = \mathbf{B}^n C^n. \tag{2}$$

Finally, when we want to return to the original resolution, we can recombine the details and the low resolution data using:

$$C^n = \mathbf{P}^n C^{n-1} + \mathbf{Q}^n D^{n-1}. \tag{3}$$

The low resolution approximation, C^{n-1}, contains low-frequency data from the original data, and can be considered equivalent to an approximation of the original input data. The details, D^{n-1}, contain the high-frequency information extracted from the original data, and can be considered equivalent to the characteristics, or features of the original data. We can use the fact that the matrices $\mathbf{A}^n$, $\mathbf{B}^n$, $\mathbf{P}^n$, and $\mathbf{Q}^n$ all have a banded regular structure in order to create a linear implementation which avoids matrix multiplication. To avoid the matrix multiplication a set of filter values from each matrix are used for the decomposition and reconstruction steps: $\left[-\frac{1}{4}, \frac{3}{4}, \frac{3}{4}, -\frac{1}{4}\right]$, $\left[\frac{1}{4}, -\frac{3}{4}, \frac{3}{4}, -\frac{1}{4}\right]$, $\left[\frac{1}{4}, \frac{3}{4}, \frac{3}{4}, \frac{1}{4}\right]^T$, $\left[-\frac{1}{4}, -\frac{3}{4}, \frac{3}{4}, \frac{1}{4}\right]^T$, are the filter values for the matrices $\mathbf{A}^n$, $\mathbf{B}^n$, $\mathbf{P}^n$, $\mathbf{Q}^n$ respectively [Samavati and Bartels 2000].

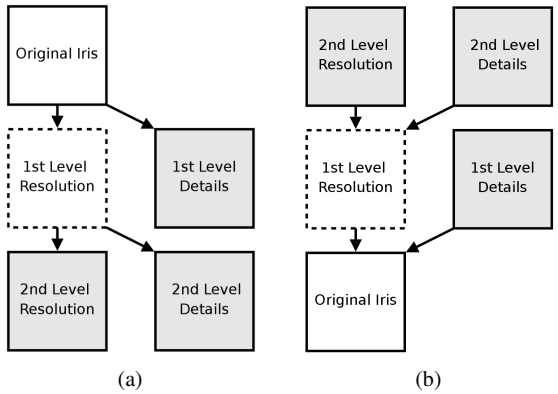

Figure 1: (a) Iris image decomposition process. (b) Iris image reconstruction process. The reconstruction process only requires the low resolution approximation and each level of details extracted during the decomposition process in order to fully recreate the original iris.

In the case of an iris image, I^n, the filters are simultaneously applied to all of the rows of the image. We can denote the row operations using the same equations (1), (2), and (3), but substituting I for C, giving us:

$$I_j^{n-1} = \mathbf{A}^n I_j^n, \tag{4}$$

$$D_j^{n-1} = \mathbf{B}^n I_j^n, \tag{5}$$

and

$$I_j^n = \mathbf{P}^n I_j^{n-1} + \mathbf{Q}^n D_j^{n-1}. \tag{6}$$

where I_j^n represents row j of the iris image at resolution level n, and D_j^n represents the corresponding details of row j. This operation results in both an intermediate representation of the image and the corresponding details obtained from reducing the resolution of each row. The filters are then applied to all of the columns of the intermediate representation. This results in a coarse approximation of the original image and two sets of details corresponding to the columns and the rows respectively. These two sets of details are stored and manipulated as one and are referred to as D^n throughout the rest of the paper. This process can be repeated several times as needed. Figure 1 gives a visual overview of both the decomposition and reconstruction process. The iris image obtained through the reconstruction process is an exact copy of the original iris image.

3 Image Databases

There are currently three publicly available databases of iris images: CASIA [CASIA 2004], UPOL [Dobeš and Machala 2005],

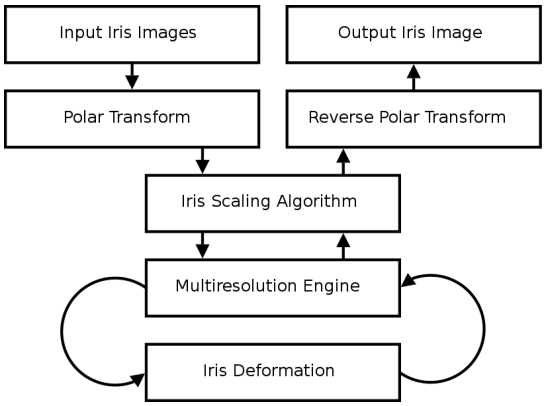

Figure 2: The preprocessing stages, and subsequent multiresolution engine organization.

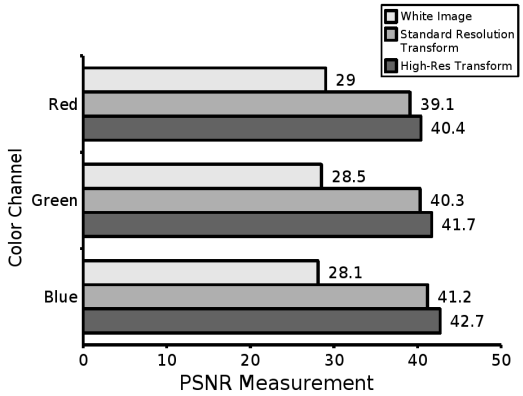

Figure 3: Chart of the PSNR measurements used to test the two polar coordinate transforms.

and UBIRIS [Proença and Alexandre 2005]. Each of the three databases has distinct characteristics, CASIA contains black and white images of medium resolution, UPOL contains color images of high resolution, and UBIRIS contains color images of high resolution as well as noisy images. Our method uses the existing images in the database to synthesize new images, therefore our output images are of the same color space and quality of the input iris images which, in turn, affects our decision of which iris database to use. Although UBIRIS is the largest public and freely available iris database, it purposefully contains many noisy iris images for testing purposes which proves unsuitable for our purposes. The CASIA database images are black and white which increases the difficulty of visual inspection of the synthesized images. Therefore we chose the UPOL database which contains high-quality, high-resolution iris images that aid visual inspection as well as remove the need to detect and avoid noisy input images.

4 Preprocessing: Isolating the iris

We use a number of preprocessing steps based on similar iris recognition methods to rid the image of extraneous information resulting in iris images like those in Figure 4. First, all of the images are edited such that the center of the image corresponds to the center of the pupil which significantly reduces the complexity of the following algorithms. Then we transform the iris into the polar coordinate system which unwraps the circular iris information into columns and rows. Next we remove the pupil to guarantee that we are working with only the iris information needed for the synthesis components of our method. Finally, once an image has been synthesized, we re-insert the pupil information and return the iris to it's natural coordinate system. The sequential organization of the preprocessing stages and subsequent synthesis framework are provided in Figure 2. We explain each of the preprocessing stages in detail in the following sections.

4.1 Polar Coordinate Representation: Unwrapping the Iris

The iris is a circular, pigmented portion of the eye, which functions to regulate the amount of light allowed to pass through to the retina. This circular nature of the iris lends itself to an alternate coordinate system. Therefore, we use a polar coordinate transform to effectively *unwrap* the iris image into a rectangular shape, resulting in the image in Figure 4(a).

Each input image is a uniform sampling of the light reflecting off of an iris. The image resulting from the polar coordinate transform represents a uniform sampling in the angle and radius axes. However, the cartesian and polar sampling rates are not equivalent; the cartesian sampling of the outer edge of the iris represents a much higher sampling rate in the angle axis than the the inner edge. In order to capture all of the details of the iris, we use a higher resolution polar coordinate representation that is large enough to contain the unwrapped circumference of the iris. The circumference of any circle is π multiplied by the diameter; in our case, w_i, the diameter of the iris is approximately the width of the image. Therefore the resulting image size must be at least πw_i; however digital images use integer sizes, hence we round π to the integer 4 which results in a polar coordinate image with dimensions $4w_i \times 4w_i$. The inverse transform reverses this process, producing an iris image in the cartesian coordinate system that is the same size as the input image.

To test this high-resolution transform we used the standard Peak Signal to Noise Ratio (PSNR) measure [Netravali and Haskell 1995]. PNSR compares an original signal to a modified version and provides a ratio of the clarity of the original signal to the introduced noise. We use the following definition of PSNR:

$$20.0 \log_{10} \left(\frac{255.0}{\sqrt{\frac{\sum \left([f(i,j) - F(i,j)]^2 \right)}{N^2}}} \right) \tag{7}$$

In our case, the original iris image, f, is compared to F, the image obtained by applying the polar transform followed by the inverse polar transform. We use our high resolution polar transform and compare it's PSNR value with that of a standard resolution transform which uses a polar coordinate image size of $w_i \times w_i$. Although it is straightforward to tell that an increase in the PSNR value represents a decrease in the noise present, PSNR is by nature a relative measurement. Consequently, we need to compare the results with a known result. For this purpose we also compared a completely white image, the equivalent of extreme noise, to the original iris image and recorded the resultant PSNR. The chart in Figure 3 clearly demonstrates that the high resolution polar coordinate transform

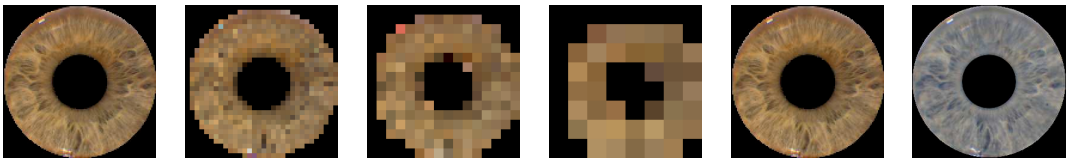

(a) (b) (c) (d) (e) (f)

Figure 5: (a) Original iris. Coarse approximation after (b) two, (c) three, (d) and four levels of reverse subdivision. The third level still contains pattern information, while the fourth level contains only color information. (e) Original iris image, compared with details (f) captured from four levels of reverse subdivision.

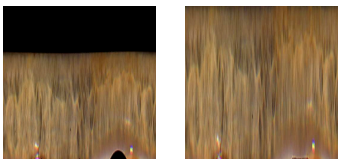

(a) (b)

Figure 4: Iris images after the preprocessing steps, (a) after being unwrapped with the polar coordinate transform, and (b) after being scaled using piecewise linear scaling algorithm.

provides a significant improvement in the quality of the resulting image.

4.2 Removing The Pupil: Iris Scaling

The size of the central portion of the iris, the pupil, is dependant upon each person and the amount of light available. In addition, the pupil may not be centered in the iris. Both of these conditions produce abnormalities in the resulting images, see Figure 4(a). The variability of the pupil size causes the variable sized black strip in the top of the resulting image. Additionally, there may exist small filled parabolas along the bottom of the image due to non-centered pupils. In order to isolate the iris we remove this extraneous information by searching each column of the image for the edges of the iris and scaling this portion of the column to fit the entire column, resulting in the image in Figure 4(b). The image is then ready to be used in the combination algorithm to produce the new iris image. Once the algorithm is finished, the new iris image must be post-processed once more to return it to the original shape and size of a real iris, see Figure 2. For this iris scaling algorithm, we needed an efficient algorithm which would allow us to both enlarge the iris and then shrink it with minimal distortion. In most cases our experimental results indicated that we would be increasing the size of the iris by about 133% and then shrinking it by 75% in the reverse process. For these purposes we chose the piecewise linear scaling algorithm [Verth and Bishop 2004] which re-samples the original information to the desired number of samples. The scaling algorithm maps the index of each pixel in the scaled column into the domain of the original column using a standard parametric representation. The resulting index is a real number, therefore, a linear interpolation is used to obtain the final color of each pixel in the scaled column. Although the re-sampling is not a reversible process, it provides an excellent representation of the original columns after both the enlarging and subsequent re-shrinking stages.

For each column, the edges of the desired iris information are first detected, and the enclosed information is then scaled. Edges of the iris are detected by finding the first pixel from the top, and the first pixel from the bottom which is not black. The comparison is performed using a given threshold, which is found by analyzing the pupils in the given database to determine their typical color. For the pre-processing, the iris information within each column is scaled to fit the full height of the image. During the post-processing the information is scaled to a fraction of the original height. The size used during the post-processing step is variable and allows the creation of irises with varying sized pupils as is found in reality under variant lighting conditions.

5 Iris Synthesis: Combining Multiple Iris Images

Our goal is to be able to augment existing iris image databases through an image synthesis process. The synthesized images should display similar characteristics to real irises, yet be unique. To achieve the goal of realism we introduce a method which combines portions of real iris images. For the goal of uniqueness our method uses multiple differing irises.

Looking at any iris image, it becomes obvious that most of its characteristics are made of high frequency data. Therefore, we employ the multiresolution techniques to capture these details from the iris. Experimental results, shown in Figure 5, demonstrate that only four levels of decomposition are required to effectively capture all of the details from a 256x256 iris image. The low resolution approximation which is left after four levels of decomposition contains only the global color scheme of the given iris. To demonstrate this observation, we decomposed an iris image and replaced it's low resolution approximation with a solid grey image. We then restored it to its original resolution, resulting in the grey iris in Figure 5(f). The new iris is simply a grey-scale version of the original iris image. This is not an interesting result, as the same effects could be achieved by employing a color-space deformation to the original image. However, the observation that the details extracted during four levels of decomposition completely capture the characteristics of an iris image is central to the combination algorithm. This observation allows us to completely decompose an iris image into the following five components: the base color of the image and the four sets of characteristics at each resolution level denoted by: I^{n-4}, D^{n-1}, D^{n-2}, D^{n-3}, and D^{n-4} respectively.

5.1 Selecting iris images to combine

As is noted, any 256x256 iris image can be decomposed into five new components. The reverse is also true, a new 256x256 iris image can be created from these same five components, due to the properties of multiresolution. For each new synthesized iris image, we select the five necessary components from those available to us in the original database. As a way of synthesizing new unique iris images, each of the components can be selected from a different

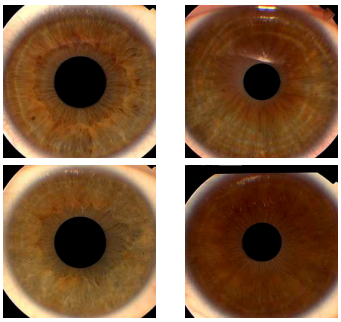

(a) (b)

Figure 6: Classifications of iris images, (a) with two rings of similar frequency characteristics and (b) with one ring of similar frequency characteristics.

iris. Given a database of N input images, we can decompose each of these images into their five components. Therefore, when synthesizing an iris image, we have N choices available for each of the necessary components which allows us to create a total of N^5 possible combinations. The original N iris images are included in these new combinations, as they are recreated when each of the selected components is from the same iris image. Clearly, given even a reasonable small database to start with, our method can generate an exponential increase in size.

To fully test our implementation of this method, we needed to consider each synthesized iris image individually in terms of quality. We also needed to test the method's ability to significantly increase the number of images in a particular database. However, as the number of output images increases, our ability to individually consider each output image significantly decreases. Therefore, we decided to not generate the exhaustive set of possibilities. Rather we generate a smaller subset which exhibits similar characteristics to the entire set. To achieve this goal we exclude the component used as the base color from the selection process, reducing the possibilities to N^4. The component to be used for the base color information is then selected uniformly from the original set of irises, which provides an even distribution of the color schemes amongst the generated irises. Next, we use only the unique combinations of the remaining four components, rather than the ordered permutations. This further reduces the number of images to the unique combinations of four iris images chosen from N. In our case, each database will contain 128 iris images. Even with the reduced number of possibilities, using our method on a database of this size will generate approximately 10 million iris images. To reduce this to a reasonable number, we separate each database into groups of eight images, and consider each group as a separate database. With each of these databases we obtain 70 new iris images from unique combinations of four irises from eight. Therefore, the total number of iris images synthesized is reduced to:

$$\frac{N}{8} \times 70, \tag{8}$$

or in our case: 1120 synthesized irises.

5.2 Classifying irises images

Fingerprints have well known classifications which allow the fingerprint generation algorithms to target a much smaller subset of the full range of possibilities. Similar to that approach, we propose two criteria for classifying irises which allows us to separate the irises into groups of similar types and subsequently improve the quality of the results.

First, we define the number of concentric rings of differing iris details within an iris. Next, we classify each of these rings by the frequency of their details; specifically we classify rings into those with high frequency characteristics and those with low frequency characteristics. Finally, in order to choose iris images which are to be combined, we group the irises into groups which contain the same number of rings and the corresponding rings contain similar frequency characteristics. An example is provided in Figure 6, where we demonstrate two different classes of irises.

Once one set of iris images have been classified, the possible combinations of irises which can be made from this small set is very large. If, for example, only 8 iris images are available, a possible $8^5 = 32768$ images can be created. Although it would be possible to automate the classifications, the combinatorial possibilities of this method make this automation a secondary goal. A user need only obtain a small number of similar iris images which can be chosen by any iris expert, and then the user is able to synthesize a database large enough to satisfy their needs.

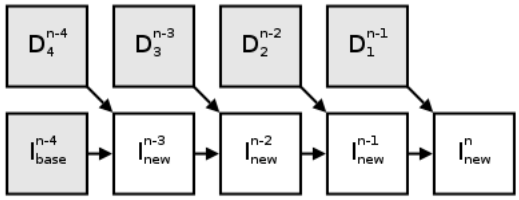

Figure 7: Structure of the combination algorithm.

5.3 Combining the details to form a new iris

Our combination algorithm requires five images from the database as input; using the subscript notation to identify each of the five images we have: I_{base}, I_1, I_2, I_3, and I_4. From these images we extract the five necessary components to build a complete iris image. First, the base color information for the new iris image I_{new}^{n-4}, is directly extracted from I_{base} by using the low resolution approximation of I_{base}: I_{base}^{n-4}. Then the characteristics, D_4^{n-4}, D_3^{n-3}, D_2^{n-2}, D_1^{n-1} are each extracted from one of the other four images. The process starts by combining the base color information, I_{new}^{n-4}, with the lowest resolution set of details, D_4^{n-4}, which results in a new, intermediate resolution iris image, I_{new}^{n-3}. Similarly, we obtain the higher resolution images, I_{new}^{n-2}, I_{new}^{n-1}, and I_{new}^{n} by iteratively applying (6):

$$I_{new}^{j} = \mathbf{P}^j I_{new}^{j-1} + \mathbf{Q}^j D_{n+1-j}^{j-1} \quad j = n-2, n-1, n \tag{9}$$

Figure 7 provides a visual layout of the composition of the new iris image. The use of details from multiple real iris images provides the synthesized iris with both a unique and realistic combination of characteristics as contained in the real irises.

6 Experimental Results

In order to test the method we selected two sample databases of irises from the existing UPOL database. The first database consisted of all of the UPOL images with duplicates removed; leaving

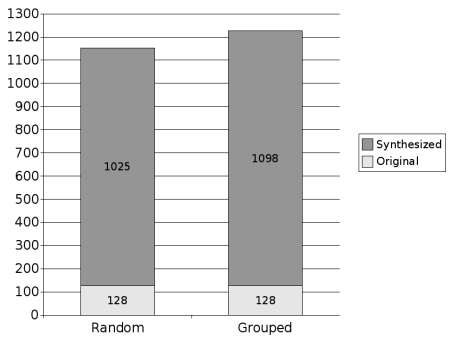

Figure 8: Original database size and the increase provided by our augmentation method.

Database	Irises Created	High Quality Irises	Ratio
Complete UPOL	1120	1025	91.5%
Grouped UPOL	1120	1098	98.0%

Table 1: The quality results of the method with the Complete UPOL database as input, and with the Grouped UPOL database as input.

a total of 128 iris images. We named this database *Complete*. The second database is a copy of the first database but is separated into two groups. The first group contains the irises which have two rings of distinctly different characteristics and the second group contains the irises which have one ring of characteristics. We called this second database *Grouped*; it also consists of 128 iris images. Our method was then used to augment each of these two databases; as noted in Section 5.1 each database was augmented with 1120 synthesized iris images. Next the synthesized iris images were examined and rated according to the clarity and realism of the characteristics as well as the uniqueness of the synthetic iris when compared with those used to create it. This visual process required that we learn the patterns and characteristics found in the real irises from the database in order to be able to distinguish the sometimes subtle differences between two similar irises. Although it is not obvious at first glance, selecting which irises to use when creating a new iris is an important step in the process. Results show that the classification process improves the overall quality of the synthetic irises, as seen in Table 1.

Figure 9 contains an example synthesized iris image with the five iris images used to create it. The synthesized image displays similar characteristics and color patterns to the real irises and thusly is a very realistic iris image. Also, it is significantly different from each of the irises used to create it and therefore is a unique iris image which can be used in addition to the existing irises in the database.

In Figure 11, we display a set of eight iris images taken from the UPOL database, alongside 16 iris images which were created from various combinations of the eight. Not only does the algorithm produce excellent individual results, but it can significantly increase the number of unique iris images contained in the database as the chart in Figure 8 demonstrates. Our implementation did not generate an exhaustive set of possible irises for logistical reasons, yet still made a significant increase to the UPOL database by providing 1098 new iris images.

7 Conclusion and Future Work

In this paper we have presented a novel method to augment existing iris image databases through iris image synthesis. We showed how the complete characteristics of an iris image can be extracted using multiple levels of reverse subdivision multiresolution. Then we provided a new method for iris image synthesis based on combining various levels of iris characteristics extracted from multiple real iris images. Next, we proposed criteria for classifying iris images in order to improve the results of the method. Finally we provided experimental results obtained using our method which demonstrate it's effectiveness at synthesizing individual iris images and increasing the size of the UPOL iris image database.

Our method will benefit from investigation into algorithmic approaches to classifying sample irises, by allowing any user who is unfamiliar with iris images to easily extend their iris image databases. Although as mentioned previously, the method's ability to exponentially increase the size of a database reduces this requirement significantly.

In order to better test iris recognition algorithms, a number of image transformation steps can be added to our post processing stages. These steps, when combined with iris scaling algorithm, can be used to produce multiple samples of the same iris with varying rotations, pupil sizes, and noise levels. This will allow our method to produce image databases similar to the UBIRIS database where multiple samples of varying quality exist for each iris.

Finally, very little work has been done on verifying synthetic biometrics. Visual inspection of iris images may be adequate if the inspection is done by an expert on iris images, however in many cases an automated verification method is desired. Statistical methods show promise, but without large databases of real samples from which to build the statistical model, the model will be biased to the samples used in it's creation. Investigation should be done into the validity of statistical biometric data verification, followed by investigation into novel, automated iris image verification methods.

References

BARTELS, R. H., GOLUB, G. H., AND SAMAVATI, F. F. 2004. Some observations on local least squares. *Scientific Computing and Computational Mathematics Program(SCCM)*.

CAPPELLI, R., MAIO, D., AND MALTONI, D. 2002. Synthetic fingerprint-database generation. In *Proc. 16th International conference on Pattern Recognition*, vol. 3, 744–747.

CASIA. 2004. Chinese academy of sciences, institute of automation. In *Casia iris image database, http://www.sinobiometrics.com*.

CUI, J., WANG, Y., HUANG, J., TAN, T., AND SUN, Z. 2004. An iris image synthesis method based on pca and super-resolution. In *Prc. of the 17th International Conference on Pattern Recognition*, IEEE Computer Society.

DAUGMAN, J. 2004. How iris recognition works. *IEEE Trans, CSVT 14*, 21–30.

DOBEŠ, M., AND MACHALA, L. 2005. Iris database. In *http://www.inf.upol.cz/iris/*.

HUANG, Y., LUO, S., AND CHEN, E. 1997. An efficient iris recognition system. In *Proc. of the IEEE*, 1348–1363.

LEFOHN, A., CARUSO, R., REINHARD, E., BUDGE, B., AND SHIRLEY, P. 2003. An ocularist's approach to human iris synthesis. *IEEE Computer Graphics*, 70–75.

NETRAVALI, A. N., AND HASKELL, G. G. 1995. *Digital pictures: Representation, Compression, and Standards*, 2nd ed. Plenum Press, New York.

PROENÇA, H., AND ALEXANDRE, L. A. 2005. Ubiris: A noisy iris image database. In *Proc. 13th ICIAP 2005 - International Conference on Image Analysis and Processing*.

SABOURIN, R., CORREIA, S. E. N., AND DE CARVALHO, J. M. 2002. On the performance of wavelets for handwritten numerals recognition. In *Proc. 16th International conference on Pattern Recognition*, vol. 3, 127–130.

SAMAVATI, F. F., AND BARTELS, R. H. 1999. Multiresolution curve and surface representation by reversing subdivision rules. *Computer Graphics Forum 18*, 2, 97–120.

SAMAVATI, F. F., AND BARTELS, R. H. 2000. Reversing subdivision rules: Local linear conditions and observations on inner products. *Journal of Computational and Applied Mathematics 119*, 1-2, 29–67.

SAMAVATI, F. F., AND BARTELS, R. H. 2004. Local filters of b-spline wavelets. In *Proc. of International Workshop on Biometric Technologies*, 105–110.

STOLLINITZ, E., DEROSE, T., AND SALESIN, D. 1996. *Wavelets for Computer Graphics*. Morgan Kaufmann, San Francisco.

UNSER, M. A. 1997. Ten good reasons for using spline wavelets. In *Proc. SPIE, Wavelet Applications in Signal and Image Processing V*, vol. 3169, 422–431.

VERTH, J. M. V., AND BISHOP, L. M. 2004. *Essential Mathematics for Games and Interactive Applications*. Morgan Kaufmann, San Francisco.

WILDES, R., AND ASMUTH, J. 1994. A system for automated iris recognition. In *Proc. of the Second IEEE Workshop on Application of Computer Vision*, 121–128.

YANG, L. H., FENG, L., AND TANG, Y. Y. 1999. A wavelet approach to extracting contours of document images. In *Proc. of the 5th Int'l Conference on Document Analysis and Recognition*, 71–74.

YANUSHKEVICH, S., STOICA, A., SRIHARI, S., SHMERKO, V., AND GAVRILOVA, M. 2004. Simulation of biometric information: The new generation of biometric systems. In *Proc. BT2004 Int'l Workshop on Biometric Technologies*, 87–98.

ZHU, Y., TAN, T., AND WANG, Y. 2000. Biometric personal identification based on iris patterns. In *Proc. of 15th Int'l conference on Pattern Recognition*, IEEE, vol. 2, 801–804.

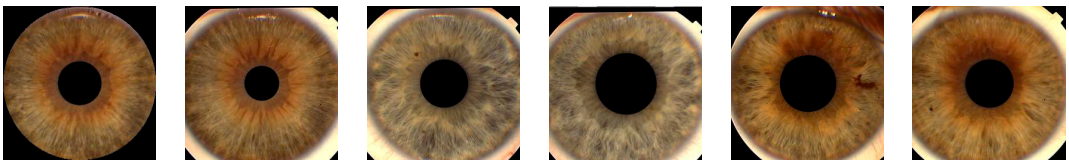

(a) (b) (c) (d) (e) (f)

Figure 9: Synthesized iris beside real iris samples used to create it. (a) The synthesized image. (b) The base iris image, I_{base}. (c)(d)(e)(f) The irises used for details, D_1^{n-1}, D_2^{n-2}, D_3^{n-3}, and D_4^{n-4} respectively.

Figure 10: A set of eight original iris images used in our algorithm.

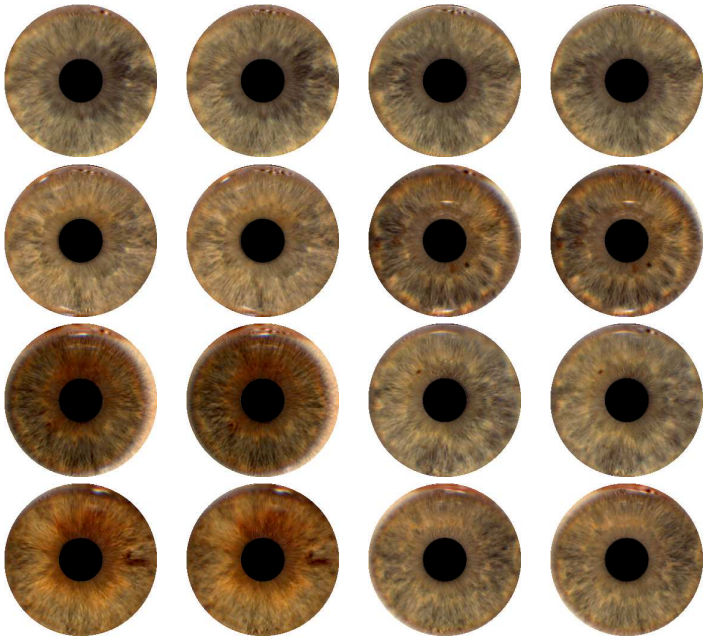

Figure 11: Synthetic iris images generated by our algorithm using combinations of the original iris images in Figure 10.